The World is Not Flat: Wireless Communications in 3D Environments

Jad Nasreddine*+, Janne Riihijärvi*, Andreas Achtzehn*, Petri Mähönen*
*Institute for Networked Systems, RWTH Aachen University, Aachen, Germany
+Mobinets, Tripoli, Lebanon

***Abstract*—Wireless network deployments are becoming increasingly complex in order to cope with the exponential growth in mobile data traffic. Multi-tier technologies capable of supporting spatially dense networks enable high data rates, but require timely and accurate models of the radio environment, particularly for scenarios that incorporate dynamic access to spectrum. However, network planners, algorithm designers, and policy makers are often forced to rely on a small set of radio propagation scenarios, often assuming fixed receiver antenna heights (RAHs). In this paper we show that the RAH in fact plays a key role not only in terms of reception quality but also in determining the interference originating from other transmitters. Our extensive simulation studies show a large variability in key performance metrics of realistic wireless network topologies as RAH is varied, which are not captured through the current practice of selecting few effectively two-dimensional scenarios and drawing general conclusions from them. These results underline the importance of adopting more realistic assumptions on RAH for design, assessment, and policy making for wireless communication systems, and the need for new propagation models valid for a wider range of RAH values than models currently in use.**

I. Introduction

Timely and accurate control of interference is crucial for wireless networks with spatially dense deployments. Emerging paradigms such as Dynamic Spectrum Access (DSA) [1] and new wireless network architectures that incorporate a vast number of devices, e.g. femtocells [2], require sufficient knowledge of the radio environment in order to achieve acceptable performance despite high spectral load. Accurate modelling of radio propagation for the purpose of quantifying interference is thus a key component of every modern wireless communication system. Consequently, imperfections in the propagation models (see, e.g. [3]–[5] for discussion) can cause poor performance and user dissatisfaction.

Besides its relevance to the performance analysis of large-scale wireless networks, propagation modelling is also starting to attract more attention from the regulatory point of view. However, regulators have so far rarely stipulated the use of more sophisticated models that would allow to integrate more details on the underlying environment and transceiver characteristics Although the ITU has published a large number of recommendations on propagation models (e.g. [6]–[8]), policy assessments are mostly limited to a small set of essentially two-dimensional "standard" radio configurations. In particular, Receiver Antenna Heights (RAHs) in the propagation models are typically set to a single value for all receivers, meant to reflect either typical or "worst-case" deployment scenario depending on the application. This is due to the fact that in most traditional wireless system deployments, *if not all*, the quality of the received signals at a terminal increases with the RAH. Hence, most of the scenarios cover only the presumably worst case for coverage and interference analysis, i.e., the lowest reasonable RAH. The monotonically increasing relation of interference on the RAH is due to the fact that the interferers in scenarios such as TV systems and outdoor macro cells are sufficiently far from receivers. This makes, for a fixed transmit power, the impact of the RAH insignificant as we show in this paper. However, the more sensitive the interference management is to precision of propagation estimates, as in the case of DSA and femtocells, the more the need for three dimensional models becomes a prerequisite.

Let us consider by way of example the case of TV white spaces (TVWSs), with the TV RAH assumed to be 10 m for fixed rooftop-mounted antennas [9]. When reasoning about TV system coverage only, without considering secondary interference, this assumption is unproblematic since typical propagation models predict monotonically decreasing path losses as as a function of the RAH [8]. Moreover, the neighboring towers which are classically the only potential source of interference are very far from the receivers. Hence, the lowest reasonable RAH can be used for worst-case estimates. This does *not*, however, demonstrate that the signal-to-interference-and-noise ratio (SINR) depends in such a manner on the RAHs in TVWS scenarios, even though this is often implicitly assumed [9]. The results in this paper show that for realistic deployment scenarios, the SINR estimates can have *highly complex* behavior as function of the RAHs.

Another example where only fixed RAHs are considered is the widely used model for femtocell scenario evaluation [10], where the antenna heights of terminals in indoor and outdoor environments are not considered in the propagation loss between the terminal and the macro Base Station (BS). These modeling assumptions are adequate when only macro/micro cells are deployed due to the comparatively high path loss between interferers and receivers compared

978-1-4673-5828-6/13/$31.00

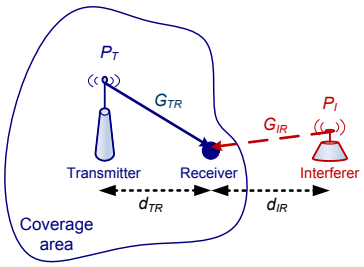

Figure 1: Simple system model composed of one transmitter, one receiver, and one interferer.

to the estimated path loss between transmitter and receiver. However, this is not the case for femtocell scenarios where a terminal inside a building connects to a femto BS in the same floor and can thus experience interference from an elevated macro BS. Considering the same propagation model as in the macrocell-only scenario will not result in worst case interference since the terminal can be more exposed to the interferer (i.e. the macro BS) when it is at higher floors.

In this paper we carry out an extensive and systematic study on the influence of the three-dimensional nature of the network structure on estimated interference. We cover some of the major propagation models proposed in the literature, including both statistical parametric models of Maciel-Xia-Bertoni (MXB) Model [11], [12], and more complex empirical models, such as the Longley-Rice Irregular Terrain Model (ITM). We derive the conditions under which non-monotonic behavior in the SINR occurs, and demonstrate how serious these effects can be in realistic scenarios. As our results demonstrate, ignoring the RAH leads to a decrease from a couple of dBs to tens of dBs in the experienced SINR by receivers. Furthermore, the protection distance of a TV system sharing its spectrum with secondary users can be incorrectly decreased by several kilometers. We also discuss the implications our results have for setting up policies for secondary use as an illustrative example, and on the need for better understanding of radio propagation characteristics considering higher RAHs than covered by existing propagation models.

The rest of this paper is structured as follows. In Section II, we describe the system model and in Section III provide a general discussion on the impact of the RAH on system performance. In Sections IV to VI we extensively study the impact of this factor. In Section VII, we discuss the main results of the paper, and propose a set of rules and requirements necessary for policy definition in future wireless networks.

II. System Model

Let us consider a simple model composed of two links as depicted in Fig. 1. These are the link carrying the useful signal from transmitter T to receiver R, and the link carrying the interference signal between interferer I and the receiver. The path gains[1] and the distances are denoted by G_{XY} and d_{XY}, where X and Y are the indices of the pair of nodes forming the link. This model can represent any wireless system considering the simple scenario of one interferer. The SINR is normally used to reflect the performance of a link. In the case of one interferer the SINR γ is given by

$$\gamma = \frac{P_T G_{TR}}{P_I G_{IR} + N_0}, \tag{1}$$

where P_T and P_I are the the transmitter and interferer powers, and N_0 is the noise power. We consider also that the transmitter has a coverage $\mathcal{C}$, inside which the SNR without the presence of interference is always higher than γ_{th}:

$$\frac{P_T G_{TR}}{N_0} \geq \gamma_{\text{th}} \qquad \forall\ R \in \mathcal{C}. \tag{2}$$

In the most common scenario, the receiver is a user terminal with unknown position (i.e. considering downlink)[2]. Hence, the impact of the interferer on system performance is usually studied considering the Worst Case Position (WCP) of the receiver, where the SINR will be the lowest possible inside the coverage area of the transmitter.

The coverage area and the WCP depend on the transmit powers, the noise power, and the path gains as it can be seen from (1) and (2). Except for the path gain, the two other factors can be determined with acceptable accuracy.

III. Impact of Receiver Antenna Heights

In order to study the impact of the RAH we shall first study the characteristics of the partial derivative of the SINR with respect to the height h. From (1) we can write

$$\frac{\partial \gamma}{\partial h} = \gamma \left[\frac{\partial}{\partial h} \ln G_{TR} - \frac{\partial}{\partial h} \ln \left(P_I G_{IR} + N_0 \right) \right]. \tag{3}$$

To the authors' best knowledge, the WCP in most of the existing works, especially related to DSA, is determined assuming the same RAH as the one used for determining the coverage area. As discussed in the introduction, in most scenarios [11]–[15], the path gain is a monotonically increasing function of the RAH since the higher the antenna less obstructions are between the transceivers. The dependency of the path gain on RAH is due, in theory, to the diffraction over the final obstruction [11], [16]. Hence, higher RAHs exhibit higher path gain. Thus, it is rational to consider the lowest antenna when determining transmitter coverage area [17]. However this is not necessary true for determining the impact of interferers, especially in scenarios where the two link environments are different. One direct counterexample is the case of a TV channel where the receiver4 is located at an elevated hill with line-of-sight (LOS) to the TV tower whereas the interferer is a mobile obstructed by

[1]The path gain is the inverse of path loss.

[2]It is the most common scenario since it includes both broadcasting and bidirectional system scenarios.

buildings. The path gain between the tower and the receiver is independent of the RAH due to LOS, whereas the one between the receiver and the interferer increases with the RAH. Thus the derivative in (3) is negative meaning that the SINR is a decreasing function of the RAH.

We will show that the SINR can be monotonically increasing, monotonically decreasing, or not monotonical at all (i.e. it can have minima and/or maxima) function of receiver antenna height, depending on the environment.

In general, propagation models can be divided into: empirical/statistical models such as the MXB model, and extended empirical models such as ITM. The former is normally used for wireless system with short to medium range such as cellular systems, whereas the latter is more suitable for systems with very large coverage areas such as TV broadcasting systems. In particular, the path gain in empirical models between transceivers X and Y is given by

$$G_{XY} = A_X A_Y g_e(d_{XY})\chi_e, \tag{4}$$

where A_X and A_Y are the gains of the antennas, $g_e(d_{XY})$ is the large scale distance-dependent factor, e reflects the environment in which the transceivers are located, and χ_e is the shadowing factor due to fixed obstacles like buildings[3]. Since antenna gains are constant, we assume that their product is equal to unity, for simplicity. In most of the models (e.g. in Hata [14], MXB [11], [12], COST-231-Walfisch-Ikegami [15], [18]) path gains can be divided into:

- Factor $L_e(d, H_X)$ that depends on distance d between the transceivers, antenna height H_X of the transmitter or the interferer X, and environment e. This factor includes A_X, A_Y, and the parts of $g_e(d_{XY})$ and χ_e that do not depend on the RAH h.
- Factor $l_e(h)$ is generally an increasing function of h for a given environment e.

This decomposition will be used to isolate the factor containing the RAH from the other factors, especially the ones depending on transmitter characteristics. More importantly, this allows us to generalize the model for the case of multiple interferers. For all these models, the factor $l_e(h)$ is the same for all interferers in case they are in the same environment (i.e. same average roof levels). This reduces the analysis complexity of the multiple interferers scenario to the case of one interferer with larger product $L_e(d, H_X)$, which intensifies the impact of the RAH on the SINR. In particular, $l_e(h)$ in Hata model does not depend on the average rooftop level and the multiple interferers case can be always reduced to one interferer case when using this model.

IV. Empirical Models without Shadowing

A. Worst Case Position

First, we shall determine the WCP for a fixed RAH. This is the position where the SINR is the lowest possible inside the coverage area. Without considering shadowing, the coverage area can be represented by a circle centered at the location of the transmitter due to the deterministic nature of the propagation losses. Moreover the path gain G_{TR} between the transmitter and the receiver is a decreasing function of distance d_{TR}, and independent of the angle. Since the interference is also a decreasing function of the distance d_{IR}, (1) shows that the WCP is the position of the receiver that minimizes d_{IR} and maximizes d_{TR}. This is, in the case of a circular coverage area, the intersection between the line joining the transmitter and the receiver, and the contour of the coverage area for each RAH. Thus the search for the WCP in the three dimensional space in this case is very easy. It requires only to find the minimum SINR over the different values of h at the intersection point aforementioned. When the shadowing factor is not considered in the empirical model, the partial derivative of γ with respect to h can be computed using (3):

$$\frac{\partial \gamma}{\partial h} = -\gamma \Bigg[\frac{\partial}{\partial h} \ln[P_I L_{e_I}(d_{IR}, H_I) l_{e_I}(h) + N_0] - \frac{\partial}{\partial h} \ln l_{e_T} \Bigg]. \tag{5}$$

The WCP in a three dimensional world for this scenario is given by the tuple (W, h_w), where W is the index of the receiver with the WCP and h_w is the RAH at which

$$h_w = \arg\min_h \gamma\big|_{R=W}. \tag{6}$$

Depending on the behavior of the derivative for the values of h ranging from the minimum RAH $h_{\min}$ to the maximum RAH $h_{\max}$, we can see, from (5) and (6), that h_w can be either $h_{\min}$, $h_{\max}$, or the solution of

$$\frac{\partial}{\partial h} \ln[P_I L_{e_I}(d_{IR}, H_I) l_{e_I}(h) + N_0] = \frac{\partial}{\partial h} \ln l_{e_T}(h).$$

B. Maciel-Xia-Bertoni Model

The MXB model [11], [12] was developed for transmitter antennas above or below average rooftop level, and a wide range of frequencies from 300 MHz to 3 GHz. The only limitation for our application is related to the height of receiver antenna that is limited to be lower than the average rooftop level (i.e. BS to BS losses are not included). In this model the path loss $1/g_e(d_{XY})$ is expressed as the product of three terms: the free-space loss L_{fs}, the multiscreen diffraction loss due to rows of buildings L_{md}, and the diffraction loss from rooftop to street L_{rts}. Only the last term depends on the RAH. In the logarithmic scale, $g_e(d_{XY})$

[3]The fast fading is not considered in this paper for simplicity, especially that for average SINR over long time the fast fading effect can be ignored.

Table I: Transmitter and receiver parameters for the MXB model without shadowing.

Parameter	h_{be_T}	H_T	b_{e_T}	x_{e_T}	N_0
Value	35 m	65 m	80 m	15 m	-109.2 dBm

can be written as function of the wavelength λ as

$$10\log g_e = 10\log \underbrace{\left[\frac{\lambda}{4\pi d_{XY}} Q_M\right]^2}_{L_e(d_{XY},H_X)} + 10\log \underbrace{\left[\frac{\lambda}{2\pi^2 r}\left(\frac{1}{\theta}-\frac{1}{2\pi+\theta}\right)^2\right]}_{l_e(h)}, \quad (7)$$

with $\theta = \tan^{-1}\left(\frac{h_{be}-h}{x_e}\right)$, and $r = \sqrt{(h_{be}-h)^2 + x_e^2}$, where x_e is the horizontal distance between the receiver and the diffracting edge, and h_{be} is the average rooftop level in environment e. The term Q_m has different values depending on the sign of $H_X - h_{be}$. In this paper we consider the case where the transmitter antenna is few meters above the average rooftop level. Therefore, Q_M is given by

$$Q_M = 2.35\left(\frac{H_X - h_{be}}{d_{XY}}\sqrt{\frac{b_e}{\lambda}}\right)^{0.9},$$

where b_e is the average distance between building rows.

From (5) and (7) we can see that the SINR behavior (the variation and not the absolute value) depends on receiver related parameters (i.e. $h_{be_I} - h$, x_{e_I}, x_{e_T} and N_0), the interferer dependent parameters (i.e. $H_I - h_{be_I}$, d_{IR}, P_I, b_{e_I}), and λ. There is no dependency on the distance dependent factor F_T or on the transmit power P_T. To study the behavior of the SINR, a TV tower transmitting with 86 dBm at frequency 522 MHz is considered. The rest of parameters are collected in Table I. We assume that the target SINR is 17.7 dB and that the frequency can be accessed in opportunistic way by a secondary interferer. The latter transmits with a power of 40 dBm and is located at 10 km from the WCP, which is 30 km away from the transmitter. The other parameters are the same as for the transmitter unless specified. The secondary is allowed to transmit if the degradation in the SINR or the coverage area does not exceed some limits.

Fig. 2 shows the SINR variation as a function of h for different values of the difference between the average rooftop levels in the two environments $\Delta h_{be} = h_{be_T} - h_{be_I}$. The figure shows that when the transmitter and the receiver have similar environments in terms of average rooftop levels, the SINR is a monotonically increasing function of h. However, this monotonicity disappears when either the buildings facing the interferer are much lower than the ones facing the transmitter or the interferer transmit power is increased. In

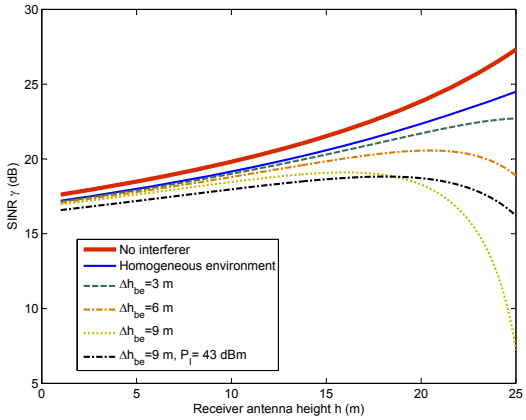

Figure 2: Variation of the SINR as a function of RAH using the MXB model for different values of Δh_{be} and P_I, and $h_{be_T} = 35$ m. The default value of P_I is 40 dBm. The red thick line is the SNR without interference and the homogeneous curve corresponds to the case where e_T and e_I are the same (i.e. $l_{e_T} = l_{e_I}$).

these cases, the SINR has a maximum at around $h = 20$ m and drops significantly when the RAH becomes closer to h_{be_I}. This is due to the faster increase in the path gain in the side of the interferer, and can be easily derived from (5) and (7). This figure clearly shows that the lowest SINR does not correspond to the lowest antenna level, but to the highest one in some scenarios[4]. These scenarios reflects the case where the heights of the building in the interferer side are lower than the ones in the transmitter side. Thus the interferer is less obstructed than the transmitter, especially when the interferer transmit power is significantly high. Hence, in scenarios where the interferer is less obstructed or has high power any policy defining interferer allowed transmit power or the required separation distance between the interferer and the receiver should use the highest possible value of h, which is the highest rooftop level.

To analyze the impact of the parameters of the transmitter environment on the estimation of the allowed transmit power, we consider a fixed coverage area with a radius of 30 km where the SNR should be equal to 17.7 dB. The power P_T is computed using the minimum RAH in the system, i.e. $h_{\text{norm}} = 10$ m [9]. To analyze the impact of considering the wrong RAH h on system performance, we estimate the transmit power of the interferer considering $h = h_{\text{norm}}$, as it is used to define policies [9]. In addition to regulators this value has been used in most of the studies on TV white space [19], [20]. Power P_I is estimated while respecting a constraint on the allowed reduction on the SINR: the reduction in the SINR at the WCP should be always less

[4]We considered that the maximum value of h is 25 m to be as close as possible to the limits given in the model. For higher values of h the SINR can drop much faster.

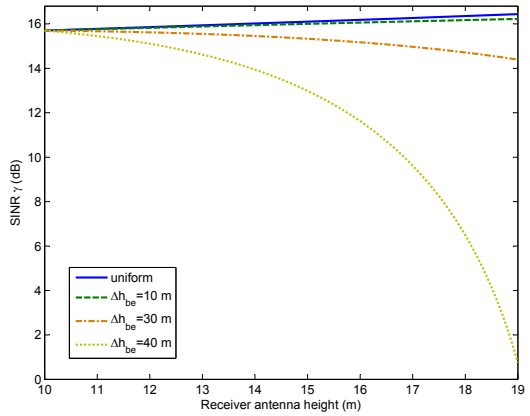

Figure 3: Variation of the SINR as a function of the RAH using the MXB model for $h_{be_T} = 60\,\text{m}$, $\delta\gamma = 2\,\text{dB}$, and different values of Δh_{be}.

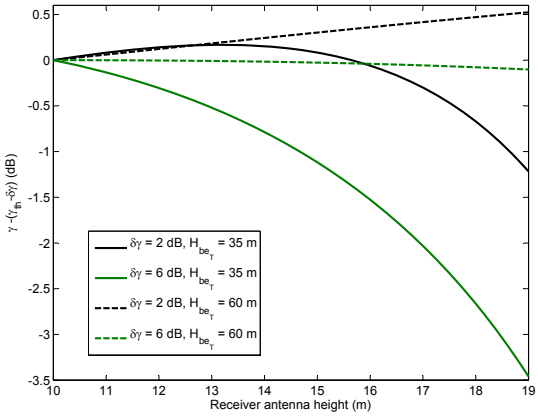

Figure 4: Variation of the SINR degradation as a function of the RAH using the MXB model for $\Delta h_{be} = 10\,\text{m}$, and different values of h_{be_T} and the allowed degradation $\delta\gamma$.

than $\delta\gamma$ dB. Using (1) the power P_I can be written as

$$P_I = \frac{1}{G_{IW}}\left[\frac{P_T G_{TW}}{\gamma_I} - N_0\right]. \tag{8}$$

where $\gamma_I = \gamma_{\text{th}} - \delta\gamma$. Using these assumptions, we analyze the impact of $\Delta h_{be} = h_{be_T} - h_{be_I}$, for an environment with two values of the average rooftop level. The results are depicted in Fig. 3 and Fig. 4. Fig. 3 shows that the degradation in the SINR, for $\delta\gamma = 2\,\text{dB}$ and $\Delta h_{be} = 40\,\text{m}$, can be as high as 16 dB especially when the difference in the average rooftop levels in the two environment is very high. This can be the case for instance when the transmitter is in a big city with skyscrapers while the interferer is in a neighboring town or a neighborhood with houses. Fig. 4 shows the degradation $\gamma - \gamma_I$ in the resulting SINR when different values of $\delta\gamma$ and H_{be_T} are considered, for $\Delta h_{be} = 10\,\text{m}$. It is interesting to see that an increase in the allowed reduction in the SINR will transform the relation between the SINR and the RAH from an increasing function to a decreasing function. Both figures show that the variation of the SINR as function of h can be modeled with monotonically increasing, concave, or simply a decreasing function depending on the considered parameters. For either low average rooftop levels or high allowed degradation, the minimum SINR is not at h_{norm}. Therefore, the estimation of the interferer power should not be estimated while considering $h = h_{\text{norm}}$ in these scenarios. These scenarios correspond to the case where the receiver can tolerate high degradation in the SINR or in cities with low average rooftop levels (e.g. below 10 floors), as for instance is the case of typical European cities.

V. Empirical Models with Shadowing

When introducing the shadowing factor, it is better to reason about the probability of unsatisfaction instead of speaking about the deterministic value of the SINR. This is due to the fact that only the distribution of the shadowing can be known in empirical models. In the following, we adopt an easy definition to the probability of unsatisfaction that allows us to analyze the impact of the RAH. We define the probability of unsatisfaction as the probability of having an SINR lower than threshold γ_I at a given position R inside the coverage area of the transmitter:

$$\mathcal{P}_R = \mathbb{P}\{\gamma < \gamma_I\}. \tag{9}$$

The objective of the network planner is to keep $\mathcal{P}_R$ lower than a threshold ε_{th}. Using (1) and (4), we can write

$$\mathbb{P}\{P_T g_{e_T}\chi_{e_T} - \gamma_I P_I g_{e_I}\chi_{e_T} \leq \gamma_I N_0\} \leq \varepsilon_{\text{th}}. \tag{10}$$

The only difference from the previous Section is that we reason in a statistical way and not in a deterministic way when determining the allowed transmit power for the interferer or the required separation distance. The interferer is not allowed to transmit if the distance to the receiver is lower than the separation distance. In case the shadowing has a log-normal distribution with zero mean and standard deviation σ, P_I can be found as a solution of (10) at the WCP. Although the approximation of $P_T g_{e_T}\chi_{e_T} - \gamma_I P_T g_{e_I}\chi_{e_I}$ with a log-normal distribution is possible, we choose here to solve this condition using numerical methods since this type of conditions will be solved off-line.

A. TV White Space Scenario

To evaluate the performance in the presence of shadowing, we consider a TV system with a coverage area of 30 km and a target SINR of 17.7 dB. The power P_T is computed to ensure that the probability of unsatisfaction in (10) is equal to 0.05 without the presence of the interferer. When the interferer is active this threshold becomes $\varepsilon_{\text{th}} > 0.05$. The other parameters are the same as in the previous section.

In Fig. 5, we show the variation of the degradation in the probability of unsatisfaction as a function of antenna receiver height when the shadowing has the same distribution in

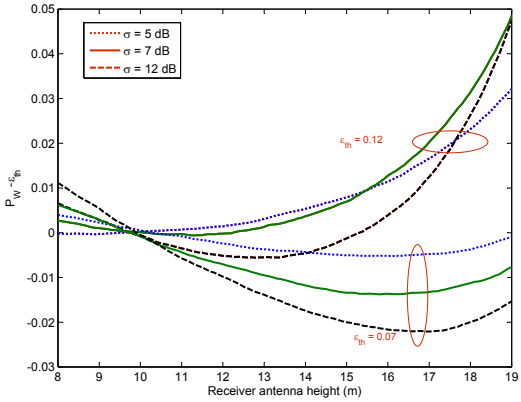

Figure 5: Variation of the degradation in the probability of unsatisfaction as a function of the RAH using the MXB model with shadowing for $\gamma_{\text{th}} = 17.7\,\text{dB}$, $h_{be_T} = 35\,\text{m}$, $\Delta h_{be} = 10\,\text{m}$, and different values of σ and ε_{th}, when the shadowing has the same distribution in both environments.

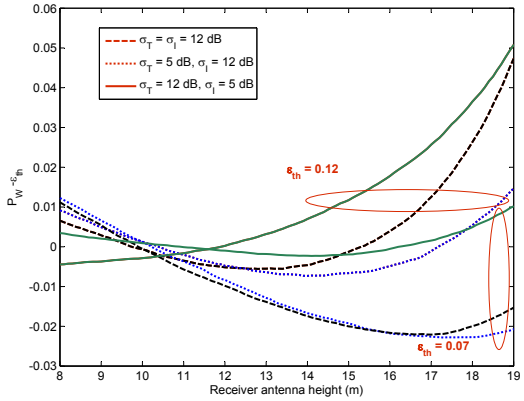

Figure 6: Variation of the degradation in the probability of unsatisfaction as a function of the RAH using the MXB model with shadowing for $\gamma_{\text{th}} = 17.7\,\text{dB}$, $h_{be_T} = 35\,\text{m}$, $\Delta h_{be} = 10\,\text{m}$, and different values of σ and ε_{th}.

both environments. The degradation is simply the difference between the probability of unsatisfaction computed when P_I is determined from (10) using $h = h_{\text{norm}}$, and ε_{th}. The figure shows that, in all cases considered in this scenario, the degradation is either a convex or a simply increasing function, and the worst RAH is not at h_{norm}, especially for high values of ε_{th}. It is important to highlight here that these results are inline with the results without considering the shadowing. Another important result is that the behavior of the degradation with respect to the shadowing standard deviation is different for low and high RAHs; the degradation is an increasing function of the standard deviation for low RAHs, whereas it is a decreasing function for high RAHs.

In Fig. 6, the same simulation is repeated but considering that the shadowing has different distributions in the two environments. It can be seen that the degradation is especially very high when the standard deviation of the shadowing in the environment of the transmitter is higher than the one in the environment of the interferer.

The conclusions in the two previous sections assume that the MXB model supports RAHs higher than 10 m. To our best knowledge there is no proof for this assumption. In general, there is a lack of measurements and studies on propagation models higher than 10 m. The conclusions in environment with shadowing are based on the assumption of having shadowing factors with static standard deviations, which does not change regardless of the distance or the RAH. However, different studies [21], [22] showed that the standard deviation depend on both of these factors. Unfortunately there is no thorough study on this dependency in the literature, and there is a clear need to develop models for it. Although exact models for high RAHs are not available, the general formulation of the SINR variation in (5) shows that the worst SINR is not always found at the lowest receiver height. The exact worst case height can be different from the ones found in the paper but the proposed procedure can be applied without loss of generality.

B. Femtocell Network Scenario

We consider also a femtocell scenario, where the femto BS can determine its transmit power depending on the interference experienced due to macro BS. The latter is located at 200 m from the receiver and transmit with 43 dBm. Building average rooftop level is 60 m and the macro BS antenna height is 90 m. The receiver is at 5 m from the femtocell and is willing to have a service with 64-QAM and a coding rate of 4/5. This requires an SINR of 22.6 dB [23]. In addition, we assume that the user is unsatisfied if this quality is provided with a probability less than ε_{th}. The shadowing standard deviations are 4 dB and 8 dB for the femto and macro BSs, respectively. We evaluate the level of the required transmit power using (10) depending on the RAH, which can be also mapped to the floor in which the femto BS is located.

In Fig 7, the required transmit power by the femto BS is plotted as a function of the RAH, which is in this case, the same as the femto antenna height. As expected, the required power increases with the increase of the RAHs, which corresponds to a decrease in the SINR for a fixed power. This is because the propagation gain in the transmitter side is independent from the RAH, whereas the one in the interferer side is an increasing function of this factor.

VI. Extended Empirical Models

Extended empirical models have their foundation in analytical wave-propagation models. They take various propagation paths and heterogeneous media into account and establish a complex framework of conditional equations to describe the impact of observable environmental and link-level parameters on the signal attenuation. Often, these

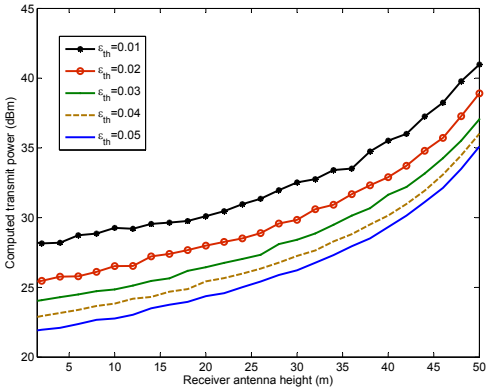

Figure 7: Required transmit power by the femtocell access point as function of the RAH, for different values of ε_{th}.

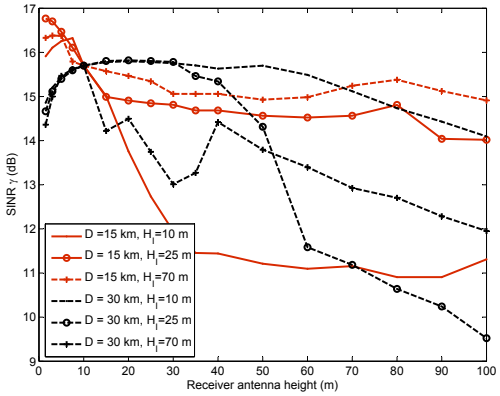

Figure 8: Variation of the lowest SINR inside the coverage using ITM model for different values of D and H_I.

models are described as correction terms that are applied to basic propagation models such as the Friis transmission equation [24]. The fine-tuning of the internal parameters of the extended empirical models require extensive measurement campaigns to cover wide input parameter ranges and a multitude of radio environments. Regression analysis and interpolation have been used to extend the applicability of the models to a set of prototypic scenarios and arbitrary combinations of input parameters. We consider one model of this family, which is widely used for TV coverage planning: the ITM [25]. The *Splat!* application [26], which incorporates a reference implementation of the model by the U.S. NTIA, enables larger studies by providing propagation estimations based on terrain data obtained in the NASA Shuttle Radio Topography Mission (SRTM) [27]. For this paper, we used Splat! to analyze the performance of a DSA system in TVWS with realistic deployment configuration. Our study incorporates the primary transmitter configuration of a single TV network operating in the area of Berlin, Germany. It consists of 4 towers broadcasting DVB-T at channel 27, i.e. a COFDM signal at a center frequency of 522 MHz and with a nominal channel bandwidth of 8 MHz. The antenna heights of the four towers are 358 m, 30 m, 195 m, and 227 m, respectively. Their individual maximum Effective Power (ERP) is 52 dBm. We have applied a common reference geometry for primary coverage calculation that assumes a roof-top mounted antenna at a height of 10 m and conservative statistical variability measures with F(95,99) [8]. The predicted signal strength is determined for a regular grid with a resolution of 250 m. We determine the coverage area of the TV towers by the contours joining points with SNR of 17.7 dB, which is the decodability threshold of the 16-QAM 2/3-modulated TV signal [17].

We chose two locations outside Berlin for the interfering secondary BS. Their distances D from the convex hull of the coverage contour are 15 km and 30 km, respectively. We varied the interferer BS antenna height and the RAH between 1.5 m and 100 m and calculated the path losses for a zone of radius 60 km around the interferer. Here, we assumed median conditions with F(50,50), which we consider a necessary generalization given additional properties of the secondary configuration, such as antenna gains, sectorization, which are beyond the scope of this paper. The transmit power of the interferer BS is determined in such way that any receiver inside the coverage zone will have an SINR higher than $\gamma_I = 15.2\,\text{dB}$ ($\delta\gamma = 2\,\text{dB}$). This distance-based method is similar to current FCC ruling for TVWS in the U.S. [28]. Using (1), the power P_I can be written as

$$P_I = \min_{R \in \mathcal{C}} \frac{1}{G_{IR}} \left[\frac{P_T G_{TR}}{\gamma_{\text{th}}} - N_0 \right]. \tag{11}$$

In Fig. 8, the impact of the RAH on the SINR at the WCP of the protection contour is depicted. Notice that the curve is highly irregular. More interestingly, the figure shows that in the case of low D the SINR is a decreasing function of h, which confirm the results obtained for the MXB model. When D is high, i.e. $D = 30\,\text{km}$, the SINR is either a decreasing function (e.g. for $H_I = 70\,\text{m}$), or a concave function (e.g. $H_I = 20\,\text{m}$), where the minimum SINR can be found for high values of h instead of the lowest value, which is normally used in the literature. Moreover, the figure shows that the degradation in the SINR can reach 6 dB, which is again an unacceptable value.

Usually, regulators specify the protection distance a secondary needs to adhere to for different RAHs and a fixed transmit power of the interferer. In a similar way, the allowed transmit power at a given protection distance s specified by regulators for different interferer antenna heights. We assume for now that the regulator wants to allow a reduction of the coverage of at maximum 5 % in the neighborhood of the interferer. In this study we consider the intersection of the disk around the transmitter location (with radius 60 km) and the contour of the TV broadcasters. The power of the interferer P_I is computed in order to guarantee this constraint considering that the RAH is 10 m, as explained

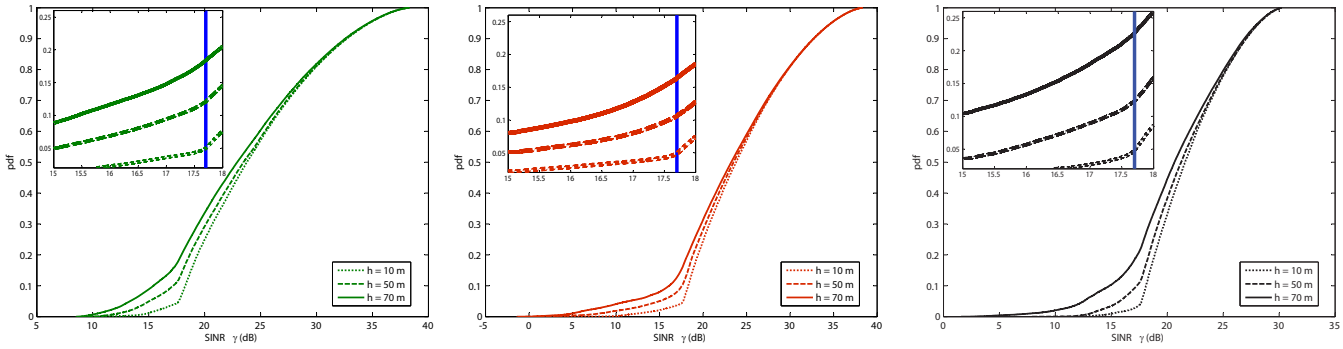

(a) Distribution of the SINR for $D = 15\,\text{km}$ and $H_I = 100\,\text{m}$.

(b) Distribution of the SINR for $D = 15\,\text{km}$ and $H_I = 25\,\text{m}$.

(c) Distribution of the SINR for $D = 30\,\text{km}$ and $H_I = 25\,\text{m}$.

Figure 9: Distribution of the SINR for different values of the distance D separating the interferer from the contour, and H_I when the ITM model is used. The small figures are zoomed versions showing the probabilities at $\gamma = \gamma_{\text{th}}$.

previously. Fig. 9 depicts the distribution of the SINR for three specific cases. The figures shows that, in this case, the coverage area will be reduced by up to 20 % in the studied area depending on interferer and the RAHs. Although the coverage reduction is only in a specific area of tens of km^2, it should be noted that this is the outage ratio when considering one interferer (secondary), and will increase in real networks where multiple interferers will appear and reduce the coverage area in the whole contour.

VII. Discussion and Conclusions

This study has shown that the SINR can be a concave, convex, monotonically increasing, or monotonically decreasing function of the receiver antenna height (RAH). Hence any study of performance, especially if dealing with worst case positions, should consider all possible RAHs. The two extreme cases from our analysis are clear. If the environment is homogeneous, or the interference level is much lower than the useful signal received, RAH does not need to be considered, whereas in the case of extended empirical models, the interference in the whole coverage area and for all possible RAHs should be analyzed. Further, there is an urgent need to develop propagation models taking into account higher receiver antennas. Although operators have sophisticated propagation tools that can work in any environment, simple models are needed for researchers and policy makers to develop simple interference models where the impact of different factors can be understood. This will enable the development of flexible techniques that can adapt their behaviors depending on the environment. Extended empirical models already allow such analysis, but they do not take environment details (e.g. buildings) into account and are not designed for small distance propagation losses.

A better understanding of the the shadowing factor behavior at different RAHs and different distances is a key requirement for the evolution of wireless networks. This includes models for the standard deviation of the shadowing that has high impact on the performance of the system as shown in this paper. In addition the correlation of the shadowing can have significant impact on interference patterns. While it is well understood that shadow correlation play key role in system performance, no three-dimensional studies of this correlation have been made to the best of our knowledge.

We conclude by highlighting the impact of our results on two key application scenarios for propagation models. Minimization of Driver-Tests (MDT) [29], a key feature of LTE-Advanced, is a method for obtaining signal and service quality measurements directly from mobile terminals. Here three dimensional location information, instead of two dimensional one, should be provided by the measurement entities due to the high impact of the RAH on propagation losses, especially for indoor environments. In DSA, the reference geometry used by regulators for estimating the allowed transmit power for the secondary systems is based on simplistic assumptions on the behavior of propagation losses. The policies normally assume a better reception with higher receiver antennas, ignoring the increase in the interference, which highly depends on terrain specifics. By considering the RAH, the complexity of generating policies on DSA by the regulator can be significantly increased. However, this complexity can be reduced by two facts. First, the variation of the propagation losses due to RAH has a limit of tens of dBs. Therefore, it is sufficient to analyze interference only for few kilometers inside the coverage area of the TV tower, instead of considering the whole coverage area. Second, receivers have normally a finite set of antenna heights corresponding to the height of building floors. Thus, a small set of propagation maps will suffice.

Overall, the aggregate errors from using models that do not consider properly terrain effects and RAHs can be very large and have direct impact on interference-limited systems. Policy makers and regulators should pay more attention to this fact, especially if the use of different spectrum access

databases that rely on propagation modeling becomes more mainstream. There is an urgent need to address this issue by developing better models and requiring their experimental validation.

ACKNOWLEDGMENT

The authors would like to thank RWTH Aachen University and DFG for providing financial support through the UMIC research centre.

REFERENCES

[1] S. Haykin, "Cognitive radio: brain-empowered wireless communications," *IEEE Journal on Selected Areas in Communications*, vol. 23, no. 2, pp. 201–220, Feb. 2005.

[2] V. Chandrasekhar, J. Andrews, and A. Gatherer, "Femtocell networks: A survey," *IEEE Comm. Magazine*, vol. 46, no. 9, pp. 59–67, Sept. 2008.

[3] A. F. Molisch, L. J. Greenstein, and M. Shafi, "Propagation issues for cognitive radio," *Proceedings of the IEEE*, vol. 97, no. 5, pp. 787 –804, May 2009.

[4] C. Phillips, D. Sicker, and D. Grunwald, "Bounding the error of path loss models," in *IEEE Symposium on New Frontiers in Dynamic Spectrum Access Networks (DySPAN 2011)*, Aachen, Germany, May 2011, pp. 71 –82.

[5] ——, "A survey of wireless path loss prediction and coverage mapping methods," *IEEE Comm. Surveys Tutorials*, vol. PP, no. 99, 2012.

[6] ITU-R, "Terrestrial land mobile radiowave propagation in the VHF/UHF bands," 2002.

[7] ITU-R, "Method for point-to-area predictions for terrestrial services in the frequency range 30 MHz to 3000 MHz (P.1546-3)," 2007.

[8] ITU-R, "Planning criteria, including protection ratios, for digital terrestrial television services in the VHF/UHF bands (BT.1368-9)," 2011.

[9] ECO WG SE43, "ECC Report 159: Technical and operational requirements for the possible operation of cognitive radio systems in the white spaces of the frequency band 470-790 MHz," 2011.

[10] Alcatel-Lucent, picoChip Designs and Vodafone, "Simulation assumptions and parameters for FDD HeNB RF requirements," R4-092042, 3GPP TSG-RAN Working Group 4 (Radio meeting n51), San Francisco, CA, May 2009.

[11] L. Maciel, H. Bertoni, and H. Xia, "Unified approach to prediction of propagation over buildings for all ranges of base station antenna height," *IEEE Trans.on Veh. Tech.*, vol. 42, no. 1, pp. 41–45, 1993.

[12] H. H. Xia, "A simplified analytical model for predicting path loss in urban and suburban environments," *IEEE Trans. on Veh. Tech.*, vol. 46, no. 4, pp. 1040 –1046, Nov. 1997.

[13] C. Q. Hien, J.-M. Conrat, and J.-C. Cousin, "Propagation path loss models for LTE-advanced urban relaying systems," in *IEEE International Symposium on Antennas and Propagation (APSURSI 2011)*, Jul. 2011, pp. 2797–2800.

[14] M. Hata, "Empirical formula for propagation loss in land mobile radio services," *IEEE Trans. on Veh. Tech.*, vol. 29, no. 3, pp. 317–325, Aug. 1980.

[15] T. Sarkar, Z. Ji, K. Kim, A. Medouri, and M. Salazar-Palma, "A survey of various propagation models for mobile communication," *IEEE Antennas and Propagation Mag.*, vol. 45, no. 3, pp. 51 – 82, june 2003.

[16] F. Ikegami, T. Takeuchi, and S. Yoshida, "Theoretical prediction of mean field strength for urban mobile radio," *IEEE Trans. on Antennas and Propagation*, vol. 39, no. 3, pp. 299–302, mar 1991.

[17] ETSI EN 300 744 V1.6.1, "Digital Video Broadcasting (DVB); Framing structure, channel coding and modulation for digital terrestrial television," Jan. 2009.

[18] COST-Action-231, "Evolution of land mobile radio (including personal) communications, final report," ETSI TR 101 112 v3.2.0, 1999.

[19] K. Harrison, S. Mishra, and A. Sahai, "How much white-space capacity is there?" in *IEEE Symposium on New Frontiers in Dynamic Spectrum (DySPAN 2010)*, Apr. 2010.

[20] J. van de Beek, J. Riihijärvi, A. Achtzehn, and P. Mähönen, "TV White Space in Europe," *IEEE Trans. on Mobile Computing*, vol. 11, no. 2, pp. 178 –188, Feb. 2012.

[21] S. Saunders and B. Evans, "The spatial correlation of shadow fading in macrocellular mobile radio systems," in *IEE Colloquium on Propagation Aspects of Future Mobile Systems*, Oct. 1996, pp. 2/1–2/6.

[22] R. Fraile, J. Nasreddine, N. Cardona, and X. Lagrange, "Multiple diffraction shadowing simulation model," *IEEE Comm. Letters*, vol. 11, no. 4, pp. 319–321, Apr. 2007.

[23] S. Sesia, I. Toufik, and M. Baker, Eds., *LTE, the UMTS Long Term Evolution: from theory to practice*. John Wiley and Sons, 2009.

[24] H. Friis, "A note on a simple transmission formula," *Proceedings of the IRE*, vol. 34, no. 5, pp. 254 – 256, may 1946.

[25] P. Rice, A. G. Longley, K. A. Norton, and A. P. Barsis, "Transmission loss predictions for tropospheric communication circuits," NBS Tech. Note 101, vols I and II., Tech. Rep., 1967.

[26] Splat! [Online]. Available: http://www.qsl.net/kd2bd/.

[27] NASA, "Shuttle radar topography mission data," ETSI TR 101 112 v3.2.0, 1999.

[28] FCC, "In the matter of unlicensed operation in the TV broadcast bands: Second memorandum opinion and order," Tech. Rep. 10-174A1, 2010.

[29] 3GPP TS 37.320 v10.0.0, "Radio measurement collection for Minimization of Drive Tests (MDT); Overall description; Stage 2," Dec. 2010.